Identification of *para*-Substituted Benzoic Acid Derivatives as Potent Inhibitors of the Protein Phosphatase Slingshot

Kang-shuai Li,[a, c] Peng Xiao,[a, b] Dao-lai Zhang,[a, e] Xu-Ben Hou,[b] Lin Ge,[a] Du-xiao Yang,[a] Hong-da Liu,[a] Dong-fang He,[a] Xu Chen,[c] Ke-rui Han,[d] Xiao-yuan Song,[f] Xiao Yu,[c] Hao Fang,[a] and Jin-peng Sun*[a]

Slingshot proteins form a small group of dual-specific phosphatases that modulate cytoskeleton dynamics through dephosphorylation of cofilin and Lim kinases (LIMK). Small chemical compounds with Slingshot-inhibiting activities have therapeutic potential against cancers or infectious diseases. However, only a few Slingshot inhibitors have been investigated and reported, and their cellular activities have not been examined. In this study, we identified two rhodanine-scaffold-based *para*-substituted benzoic acid derivatives as competitive Slingshot inhibitors. The top compound, (Z)-4-((4-oxo-2-thioxo-3-(*o*-tolyl)thiazolidin-5-ylidene)methyl)phenoxy)methyl)benzoic acid (**D3**) had an inhibition constant (K_i) of around 4 μM and displayed selectivity over a panel of other phosphatases. Moreover, compound **D3** inhibited cell migration and cofilin dephosphorylation after nerve growth factor (NGF) or angiotensin II stimulation. Therefore, our newly identified Slingshot inhibitors provide a starting point for developing Slingshot-targeted therapies.

Reversible protein phosphorylation plays an important role in controlling various cellular functions such as cell growth, differentiation, gene expression, and cellular metabolism.[1] In cells, protein kinases and protein phosphatases work together to precisely control the balance of the protein phosphorylation network to regulate different life activities. The dual-specific phosphatase Slingshots (SSHs) form a particular group of phosphatases which regulates cytoskeleton rearrangement through dephosphorylation of cofilin at its Ser-3, as well as of Lim kinases (LIMKs) at Thr-508 (LIMK1) or Thr-505 (LIMK2).[2] Because dephosphorylated cofilin mediates actin depolymerization, which is a key step in the metastasis of cancer cells as well as the entry of infectious Salmonella into mammalian cells, down-regulation of Slingshot phosphatase activity by small molecule inhibitors can be a promising therapeutic strategy for cancers or salmonella-related diseases such as mild food poisoning or life-threatening typhoid fever.[2a, d, 3]

Until now, only one report has identified several inhibitors of Slingshot 1 using virtual screening and homology modeling of the phosphatase. The best inhibitor among these compounds displays an IC_{50} of around 3 μM toward Slingshot 1; however, the inhibition mode of these compounds have not been determined, and their selectivity toward other phosphatases have not been tested. The cellular activities of these compounds have not been determined either. Thus, there is a need to develop new slingshot inhibitors with good selectivity and cellular activity to evaluate their therapeutic potential.

Recently, we have uncovered nine specific lymphoid-specific tyrosine phosphatase (LYP) inhibitors through target–ligand interaction-based virtual screening methods.[4] Based on the predicted binding modes and the structure–activity relationship analysis of these in-silico-identified LYP inhibitors, we found that the benzoic acid group could bind into the active site of LYP and contribute to the inhibitory activity against it. Considering the structural conservation of the active site of the tyrosine phosphatase superfamily, compounds containing the benzoic acid fragment might also inhibit the activity of Slingshots.

In the present study, we synthesized a series of rhodanine–benzoic acid derivatives and screened these compounds for potential Slingshot inhibitor leads. Additionally, several commercial compounds containing benzoic acid groups were selected from our previous virtual screening study and were tested for Slingshot inhibitory activities. As results, we found two rhodanine–benzoic acid derivatives are inhibitors of Slingshot 2 with inhibition constants (K_i) less than 20 μM. These inhibitors are competitive inhibitors and further studies revealed that one of the inhibitors shows selectivity toward other phos-

[a] Dr. K.-s. Li,+ Dr. P. Xiao,+ Dr. D.-l. Zhang, Dr. L. Ge, Dr. D.-x. Yang, Dr. H.-d. Liu, Dr. D.-f. He, Prof. H. Fang, [. P. J.-p. Sun
Key Laboratory Experimental Teratology of the Ministry of Education (MOE) and Department of Biochemistry and Molecular Biology
School of Medicine, Shandong University, Jinan, Shandong 250012 (China)
E-mail: sunjinpeng@sdu.edu.cn

[b] Dr. P. Xiao,+ Dr. X.-B. Hou
Department of Medicinal Chemistry
Key Laboratory of Chemical Biology of Natural Products (MOE)
School of Pharmacy, Shandong University, Jinan, Shandong 250012 (China)

[c] Dr. K.-s. Li,+ Dr. X. Chen, Prof. X. Yu
Department of Physiology, School of Medicine
Shandong University, Jinan, Shandong 250012 (China)

[d] Dr. K.-r. Han
Mailman School of Public Health
Columbia University, New York, NY 10032 (USA)

[e] Dr. D.-l. Zhang
School of Pharmacy, Binzhou Medical University
Yantai, 264003 (China)

[f] Prof. X.-y. Song
Key Laboratory of Brain Function and Disease
Chinese Academy of Sciences (CAS) and
School of Life Sciences, University of Science and Technology of China
Hefei, 230027 (China)

[+] These authors contributed equally to this work.

Supporting information for this article is available on the WWW under http://dx.doi.org/10.1002/cmdc.201500454.

phatase and effectively block the cell migration through inhibiting Slingshot activity in cells.

We first synthesized the rhodanine-scaffold-based phosphatase inhibitor library. Target compounds **D3, D17, D25**, and **D16** were prepared according to the synthetic routes as shown in Scheme 1. To synthesize target compounds, 4-substituted benzaldehydes were first prepared through coupling and/or substitution reactions. Afterwards, 3-substituted rhodanines were generated by a three-step reaction procedure. Then, the aldol reaction of the two intermediates afforded target compounds **D3**, **D17**, **D25**, and **D16**. The target compound **D1** was synthesized through a simple substitution reaction as shown in Scheme 2.

Compounds that contained a benzoic acid group were selected from our in-house compound library and screened for inhibition of phosphatase activity of the catalytic domain of Slingshot 2 (residues 233–490) (Table 1). At 50 μm, four compounds decreased Slingshot 2 activity against a small artificial substrate, *para*-nitrophenylphosphate (pNPP), by more than 20%, and two of them showed inhibition rates over 70%. These two most potent compounds were *para*-substituted benzoic acid derivatives: (*Z*)-4-((4-((4-oxo-2-thioxo-3-(*o*-tolyl)-thiazolidin-5-ylidene)methyl)phenoxy)methyl)benzoic acid (**D3**) and (*Z*)-4-((4-((3-(1-carboxy-2-(1*H*-indol-3-yl)ethyl)-4-oxo-2-thioxothiazolidin-5-ylidene)methyl)phenoxy)methyl)benzoic acid (**D17**), as seen in Figure 1 A,B. Using a fixed pNPP concentration of 11 mm (the Michaelis constant, K_M, of Slingshot 2), the IC_{50} of **D3** was determined as 8.2 ± 2.6 μm and the IC_{50} for **D17** was determined as 42 ± 6.1 μm, respectively (Supplemental Figure 1 in the Supporting Information).

To determine the inhibition modes of **D3** and **D17**, we performed Michaelis–Menten kinetic studies with recombinant Slingshot 2 using varying inhibitor and substrate concentrations. The Lineweaver–Burk plots revealed that both compounds **D3** and **D17** are competitive inhibitors of Slingshot 2 with a calculated K_i of 3.9 ± 0.3 μm and 18.9 ± 0.3 μm, respectively (Figure 1 C,D). **D3** is a reversible inhibitor and inhibits Slingshot 2 approximately fourfold better than **D17**; we therefore selected compound **D3** for further study (Figure 1 C,D and Supplemental Figure 2 in the Supporting Information).

To determine the selectivity of **D3** toward other phosphatases, we purified a panel of other protein phosphates including PTP-Meg2, PTP-N18 (BDP1), PRL-1, MKP3, PPM1A, PPM1G, and PP1. The purities of these proteins were confirmed by electro-
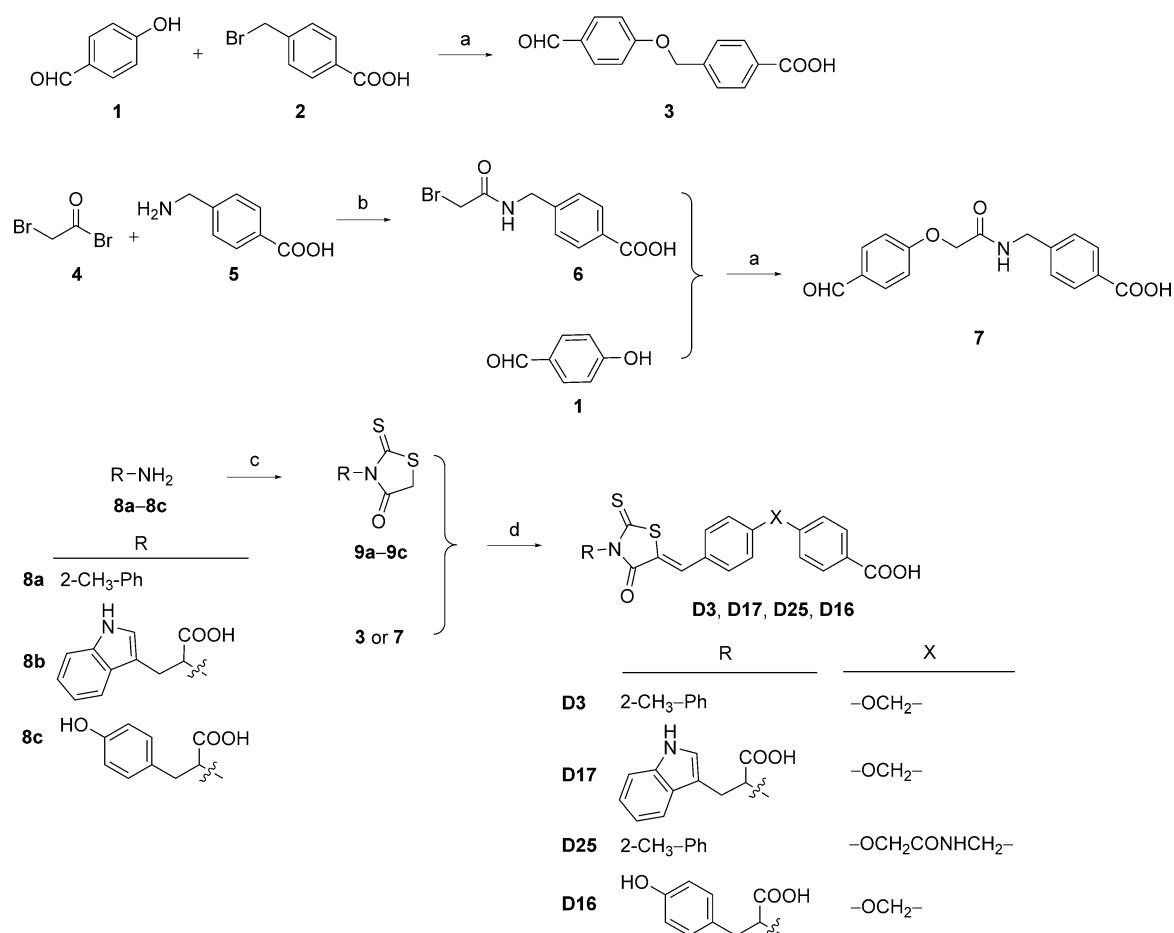
Scheme 1. Synthesis of D3, D17, D25, and D16. *Reagents and conditions*: a) K_2CO_3, acetone, reflux, 8 h, **3**: 63%, **7**: 52%; b) NaHCO_3, THF, 0 °C, 4 h, 55%; c) 1) CS_2, Et_3N, EtOH, 0 °C, 4 h, 2) ClCH_2COONa, H_2O, 0 °C, 12 h, 3) 6 m HCl, 85 °C, 4 h, **9a**: 72%, **9b**: 36%, **9c**: 47%; d) NH_4Ac, HAc, reflux, 0.5 h, **D3**: 59%, **D17**: 57%, **D25**: 68%, **D16**: 51%.
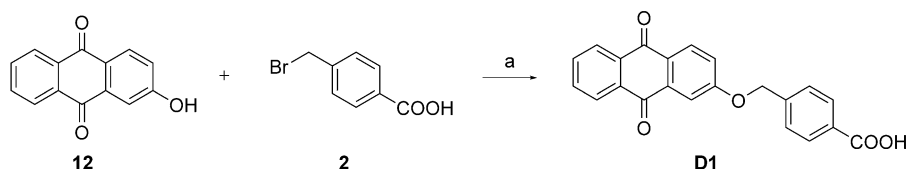
Scheme 2. Synthesis of **D1**. *Reagents and conditions*: a) K$_2$CO$_3$, acetone, reflux, 8 h, 34%.

phoresis. K_i assays were performed according to procedures described previously, and the results are shown in Supplemental Figure 3 in the Supporting Information and summarized in Table 2. Selectivity of **D3** for Slingshot 2 ranged from 2.9-fold over PPM1A and up to >12.8-fold over PPM1G and PP1. We also compared the inhibitory activity of **D3** toward Slingshot 2 and Slingshot 1, using the catalytic domain of Slingshot 2 (residues 305–450) and the catalytic domain of Slingshot 1 (residues 309–460), because longer Slingshot 1 constructs were not soluble in an *E. coli* expression system. The results indicate that **D3** has similar inhibitory activities toward both Slingshot 1 and Slingshot 2 (Table 2).

Slingshot is a cofilin phosphatase and regulates cytoskeleton dynamics through dephosphorylation of cofilin at its Ser-3 position.[1f,5] In particular, previous studies have shown that cofilin phosphorylation was significantly decreased after nerve growth factor (NGF) stimulation, and knockdown of Slingshots significantly reversed this process in a PC12 (pheochromocytoma) cell model.[6] We therefore used PC12 cells to examine the cellular activity of compound **D3** in NGF signaling. PC12 cells were preincubated with compound **D3** for 45 min and then stimulated with 100 ng mL^{-1} NGF. As shown in Figure 2, NGF-induced dephosphorylation of cofilin were significantly blocked by compound **D3** at 15 and 30 min. These results confirm that compound **D3** inhibited Slingshot activity in PC12 cells. We next examined whether **D3** regulated cofilin dephosphorylation through direct inhibition of Slingshot. In HEK293 (human embryonic kidney) cells transfected with Flag-tagged AT1R, 20 μM angiotensin II-induced cofilin dephosphorylation was specifically blocked by compound **D3** (Supplemental Figure 4 in the Supporting Information). Knockdown of both Slingshot 1 and Slingshot 2 eliminated the effect of **D3** on cofilin dephosphorylation (Supplemental Figure 4 in the Supporting Information). Therefore, compound **D3** prevented cofilin dephosphroylation through inhibition of Slingshot.

Slingshot promotes cancer cell migration and facilitates the entry of infectious Salmonella into mammalian cells by dephosphorylation of cofilin. Studies have shown that knockdown of Slingshot expression by small interfering RNAs (siRNAs) significantly decreased the lysophosphatidic acid (LPA)-induced cell migration of rat ascites hepatoma (MM1) cells and their motility in two-dimensional culture. Therefore, a Slingshot inhibitor could be developed to treat cancer cells or infectious diseases by inhibition of cell migration or occlusion of cytoskeleton dynamics.

We then examined the effects of compound **D3** in cell migration using the transwell migration assay. PC12 cells pretreat-

ed with varying concentrations of **D3** were overlaid in the upper chamber of a transwell assay plate, while NGF was present in the lower chamber as chemoattractant. After 24 h, the number of cell foci that transmigrated to the lower chamber, past the micropores of the cell-permeable membrane, was counted. Incubating cells with **D3** at 5 μM significantly decreased the NGF-induced cell migration, consistent with its inhibitory role in cofilin dephosphorylation (Figure 2 C,D and Figure 3). In contrast, the compound **A14**, which has a similar scaffold but lacks the Slingshot inhibition activity, had no effect on NGF-stimulated cell migration (Figure 3). Moreover, in HEK293 cells overexpressed AT1R, the effect of **D3** on cell migration was totally abolished by knockdown of both Slingshot 1 and Slingshot 2 (Supplemental Figure 5 in the Supporting Information). Taken together, these results confirm the cellular activity of compound **D3** in the inhibition of cell migration by targeting Slingshot. Thus, **D3** can be selected as a candidate for further antitumor drug development.

In conclusion, Slingshot phosphatases are key regulators of cell skeleton rearrangement during cancer cell migration and bacterial infection. Inhibition of Slingshot by small chemical compounds has therapeutic potential to treat cancer and certain infectious diseases. However, only few compounds have been identified to be Slingshot inhibitors in the micromolar range.[1a] The selectivity toward other phosphatases and the cellular activity of these Slingshot inhibitors reported so far have not been investigated. Therefore, the potential of these compounds as leads to develop therapeutic methods targeting Slingshot is still unknown. Here, we have identified two benzoic acid derivatives as competitive Slingshot inhibitors with K_i values below 20 μM in vitro. Biochemical and cellular studies demonstrated that the most potent inhibitor, **D3**, inhibited Slingshot-mediated cell migration in PC12 cells and showed certain selectivity toward several other phosphatases Therefore, compound **D3** is a good lead for more potent and selective Slingshot inhibitors for therapeutic applications. Future research dealing with crystallographic studies of the **D3**/Slingshot complex or structure–activity relationship studies could help us understand the structural basis of **D3**-based Slingshot inhibition and help us design better inhibitors.
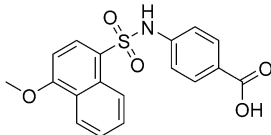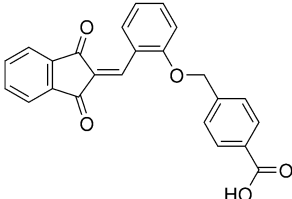
Experimental Section

Materials and equipment. pNPP was purchased from Sangon Biotech Co., Ltd. Ni-NTA agarose was from Amersham Pharmacia Biotech. Anti-cofilin/pS3 antibody was purchased from Santa Cruz. The mouse anti-GAPDH monoclonal antibody was from ZSGB-BIO Co. The NGF was purchased from Sino Biological Inc. All other chemicals and reagents were from Sigma. ^{1}H and ^{13}C NMR spectra were obtained on a Bruker spectrometer (600 and 300 MHz, Bruker Corp., CA, USA). Chemical shift values (δ) are expressed in parts per million (ppm) relative to TMS internal standard, and significant data are reported in order of multiplicity (s = singlet, d = doublet,

Table 1. Initial screening of the benzoic acid derivatives toward inhibition of Slingshot 2 phosphatase activity.

Compound	Structure	Molecular weight	Inhibition [%]
D3[b]		461.55	86 ± 5
D17[b]		558.62	75 ± 6
B7[a]		439.46	39 ± 3
D1[b]		358.34	29 ± 6
D25[b]		518.60	19 ± 3
D16[b]		535.59	15 ± 4
B16[a]		527.75	9 ± 3
A14[a]		495.94	1 ± 1
A11[a]		541.34	–
A13[a]		426.49	–

Table 1. (Continued)

Compound	Structure	Molecular weight	Inhibition [%]
B15[a]		357.38	–
B22[a]		384.38	–

The compounds are sorted by their inhibition rates for Slingshot 2. [a] Purchased from commercial sources; [b] synthesized compounds. All measurements were carried out at pH 7.0, 25 °C, in DMG buffer with enzyme concentration of 100 nM as described in the Experimental Section. All experiments were performed in triplicate and the data are expressed as mean ± SD.

t = triplet, m = multiplet) and number of protons. High-resolution atmospheric-pressure electrospray ionization mass spectrometry (HRMS (AP-ESI)) was carried out on an Agilent 6510 quadrupole time-of-flight LC–MS instrument (Agilent Technologies, CA, USA).

General procedure for the synthesis of the rhodanine-scaffold-based phosphatase inhibitor library. Target compounds **D3, D17, D25**, and **D16** were prepared according to the synthetic routes shown in Scheme 1. 4-hydroxybenzaldehyde (**1**, 0.61 g) was dissolved in acetone (100 mL). Afterwards, K_2CO_3 (2.07 g) and 4-(bromomethyl)benzoic acid (**2**, 1.08 g) were added, and the mixture was left at reflux for 12 h to get intermediate **3**. The coupling reaction of bromoacetyl bromide (**4**, 12.8 g) and 4-(aminomethyl)benzoic acid (**5**, 8.0 g) afforded **6**. After that, **7** was synthesized following the same substitution reaction as for **3**. Next, the intermediate N-substituted rhodanines **9a–9c** were prepared following the same procedure as in literature.[9] In brief, under ice-bath conditions, substituted amine (**8a–8c**, 5 mmol) and triethylamine (2.53 g) were dissolved in EtOH (1 mL) followed by dropwise addition of CS_2 (0.76 mL). The resulting precipitate was obtained by filtration and washed with water. Then it was added gradually to a solution of sodium chloroacetate (0.64 mL, 5.5 mM). After stirring overnight at room temperature, HCl (7 mL, 6 M) was added to the mixture and stirred again at 85 °C for 4 h to obtain **9a–9c**. After all the intermediates were synthesized, the target compounds **D3, D17, D25**, and **D16** were afforded through the aldol condensation reaction of **3** (or **7**) and the appropriate intermediate **9** in HOAc with the addition of NH_4OAc.[9]

As shown in Scheme 2, target compound **D1** was synthesized following a similar route as in Scheme 1.

(Z)-4-((4-((4-Oxo-2-thioxo-3-(o-tolyl)thiazolidin-5-ylidene)methyl)phenoxy)methyl)benzoic acid (D3): Yellow solid (0.14 g, 59%); mp: 276–278 °C; ^{1}H NMR (600 MHz, [D_6]DMSO): δ = 12.55 (s,1 H), 7.98 (d, J = 7.8 Hz, 2 H), 7.85 (s,1 H), 7.70 (d, J = 7.8 Hz, 2 H), 7.59 (d, J = 7.8 Hz, 2 H), 7.43 (m,2 H), 7.38 (m, 1 H), 7.34 (d, J = 7.8 Hz, 1 H), 7.24 (d, J = 7.8 Hz, 2 H), 5.33 (s, 2 H), 2.06 ppm (s, 3 H); ^{13}C NMR (100 MHz, [D_6]DMSO): δ = 192.9, 167.0, 166.7, 160.5, 141.4, 135.8, 134,3, 133,4, 133.0, 130.9, 130.4, 129.8, 129.5, 129.0, 127.5, 127.2, 125.9, 119.9, 116.0, 69.0, 16.8 ppm; HRMS (AP-ESI) m/z [M+H]+ calcd for $C_{25}H_{19}NO_4S_2$: 462.0828, found 462.0829.

(Z)-4-((4-((3-(1-Carboxy-2-(1H-indol-3-yl)ethyl)-4-oxo-2-thioxo-thiazolidin-5-ylidene)methyl)phenoxy)methyl)benzoic acid (D17): Brown solid (0.16 g, 57%); mp: 207–209 °C; ^{1}H NMR (300 MHz, [D_6]DMSO): δ = 13.07 (br s, 2 H), 10.77 (s, 1 H), 7.97 (d, J = 8.4 Hz, 2 H), 7.74 (s, 1 H), 7.60-7.56 (m, 4 H), 7.48 (d, J = 7.8 Hz, 1 H), 7.26 (d, J = 8.1 Hz, 1 H), 7.19 (d, J = 8.4 Hz, 2 H), 7.04 (m, 1 H), 7.00 (m, 1 H), 6.90 (m, 1 H), 5.85 (br s, 1 H), 5.30 (s, 2 H), 3.76 (m, 1 H), 3.61 ppm (m, 1 H); ^{13}C NMR (75 MHz, [D_6]DMSO): δ = 192.9, 168.8, 167.0, 166.6, 160.3, 141.2, 135.9, 132.9, 130.5, 129.4, 127.4, 127.1, 125.7, 123.3, 120.7, 118.2, 117.8, 115.9, 111.2, 109.7, 68.9, 23.2, 14.0 ppm; HRMS (AP-ESI) m/z [M+H]+ calcd for $C_{29}H_{22}N_2O_6S_2$: 559.0992, found 559.0993.

Constructs. The full-length human Slingshot 1 cDNA was a gift from Dr. Robert. J. Lefkowitz of Duke University (Durham, NC, USA) and have been described previously.[7] The constructs of histidine-tagged phosphatases, namely His-PPM1A, His-PPM1G, His-PRL-1, His PTP-MEG2(277-583), His-MKP3, and His-PTPN18 (catalytic domain) have been described previously.[1c, d, 8]

Protein expression and purification. The catalytic domain of Slingshot 2 (residues 305–450 and 233–490) and Slingshot 1 (residues 309–460) with an N- terminal his tag was prepared and used for in vitro studies. BL21 (DE3) E. coli cells were transformed with the expression plasmids and cultured in lysogeny broth (LB) medium with shaking at 37 °C. The culture temperature was adjusted to 18 °C at OD_{600} = 0.6, and expression was induced for 12 h with 0.3 mM isopropyl β-D-1-thiogalactopyranoside (IPTG) once OD_{600} reached 0.8. The cells were harvested by centrifugation and resuspended in lysis buffer (50 mL, 20 mM Tris pH 8.0, 150 mM NaCl). After centrifugation, the supernatant was incubated with Ni^{2+}-NTA resin with end-to-end mixing at 4 °C for 1 h. The beads were collected and washed 3 times with buffer (20 mL, 20 mM Tris pH 8.0, 150 mM NaCl, and 5 mM imidazole) and eluted with an imidazole gradient (20 mM Tris pH 8.0, 150 mM NaCl, and 20–200 mM imidazole). After purification, the protein was further concentrated by ultrafiltration and stored at −80 °C. Expression and purification of the other His-tagged proteins were performed as previously described.

Chemical library screening. The collected compounds were screened in a 96-well format. To initiate the reaction, 100 nM Sling-
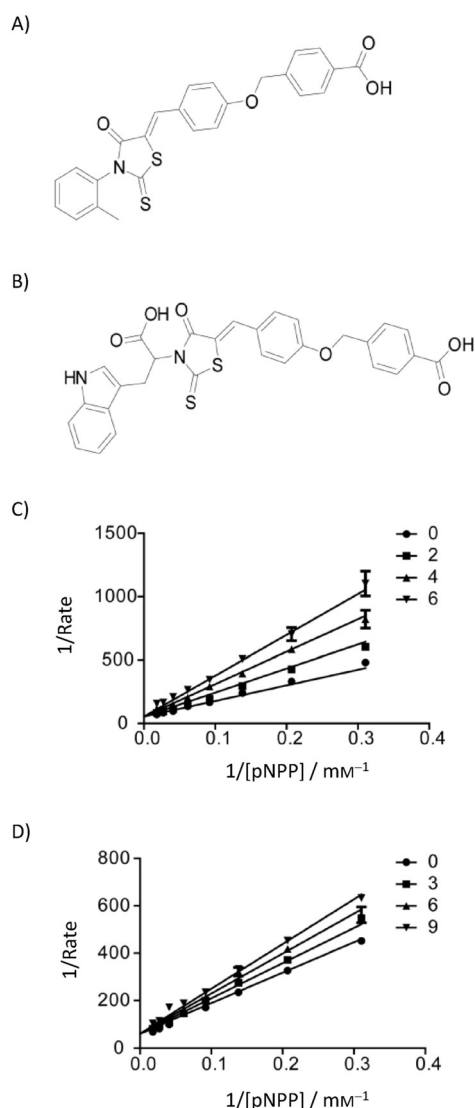
A)

B)

Table 2. Selectivity of compound **D3** toward a panel of protein phosphatases.

Enzymes	K_i [μм][a]	Ratio toward SSH2
SSH2 (233-490)	3.9 ± 0.3	1.0
PPM1A	11.4 ± 1.0	2.9
PRL-1	13.8 ± 2.0	3.5
PTPMEG2	14.6 ± 1.0	3.7
PTPN18	20.4 ± 2.3	5.2
MKP3	21.6 ± 2.7	5.5
PPM1G	> 50	> 12.8
PP1	> 50	> 12.8
SSH2 (305-450)	8.9 ± 0.7	2.3
SSH1 (309-460)	7.4 ± 0.9	1.9

[a] All measurements were assayed using pNPP as a substrate at pH 7.0, 25 °C, in DMG buffer with ionic strength adjusted to 0.15 м. All experiments were performed in triplicate, and the data are expressed as mean $\pm$ SD.

C)

D)

A)

B)

Figure 1. Chemical structures and kinetic studies of **D3** and **D17** for their inhibitory activity against Slingshot 2. A–B) Chemical structures of the two most potent compounds from the screening library. A) Chemical structure of compound **D3**. B) Chemical structure of compound **D17**. C–D) Kinetic studies of the inhibition mode of **D3** and **D17**. pNPP concentrations were 3.22, 4.83, 7.24, 10.9, 16.3, 24.4, 36.7, and 55 mм, respectively. C) Lineweaver–Burk plot for compound **D3**-mediated SSH2 inhibition using pNPP as a substrate. D) Lineweaver–Burk plot for compound **D17**-mediated SSH2 inhibition using pNPP as a substrate.
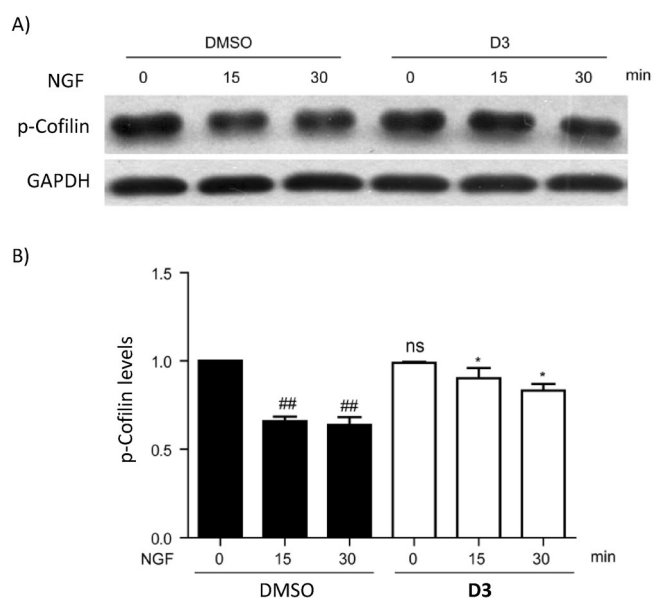
Figure 2. D3 attenuates NGF-induced cofilin dephosphorylation at pSer3 position in PC12 cells. A) Effects of compound **D3** (5 μм) on the NGF-induced cofilin dephosphorylation as detected by the anti-pS3-cofilin antibody. The GAPDH level was used as a control. B) Statistical analysis of the phosphorylation of cofilin pS3 in PC12 cells treated with NGF. All experiments were repeated in at least triplicate. ns: no significant difference was observed between DMSO and D3 treated groups. ##$p < 0.01$, NGF treated cells were compared with control cells. *$p < 0.05$; **$p < 0.01$; **D3**-treated cells were compared with DMSO-treated cells.

shot 2 was added to a 3,3-dimethylglutarate (DMG) buffer consisting of 11 mм pNPP, 50 μм compound, 50 mм DMG, pH 7.0, 1 mм EDTA, and 2 mм dithiothreitol (DTT) with an ionic strength of 0.15 м, adjusted by NaCl. The final volume for each well was 120 μL. The reaction mixture was incubated at 37 °C and continuously measured at 405 nm using a Molecular Devices EMax precision microplate reader (Sunnyvale, CA, USA). Compounds with an inhibition rate of 50 % or more were further tested for IC$_{50}$ and K_i studies. All assays were performed in triplicate.

IC$_{50}$ measurements. Kinetic assays for Slingshot 2-catalyzed pNPP hydrolysis in the presence of small-molecular inhibitors were measured as previously described.[4] The effect of each inhibitor on the Slingshot 2-catalyzed pNPP hydrolysis was determined at 25 °C in reaction buffer (50 mм DMG buffer with an ionic strength of

0.15 м adjusted by NaCl). The K_M value of Slingshot 2 toward pNPP hydrolysis (11 mм for pNPP) was used to determine the IC$_{50}$. The reaction was detected by monitoring the absorbance of pNPP at 405 nm. The IC$_{50}$ values were obtained by fitting the data to Equation (1) using GraphPad Prism 5 (GraphPad Software, Inc., La Jolla, CA, USA) as follows:

$$A_I = A_0 \times \text{IC}_{50} / (\text{IC}_{50} + [I]) \tag{1}$$

K_i measurements. The phosphatase-catalyzed hydrolysis of pNPP in the presence of inhibitors was assayed at 25 °C. The reaction
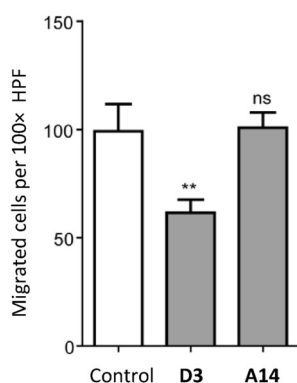
Figure 3. Compound **D3** inhibits the NGF-induced migration of PC12 cells. The transwell assay was used to examine the **D3** effects on NGF-induced cell migration. The PC12 cells were preincubated with **D3** (5 μm in 0.2 % DMSO), **A14** (5 μm in 0.2 % DMSO), or control vehicle (0.2 % DMSO) for 45 min. Approximately $1 \times 10^5 / 100$ μL cells were added to each upper chamber, and the 100 ng mL^{-1} NGF was incubated in the lower chamber as a chemoattractant. After 24 h, the number of migrated cells was counted. **p < 0.01, **D3**-treated cells were compared with DMSO-treated cells (control); ns: no significance was found between **D3**-treated cells and DMSO-treated cells (control). All statistics shown represent the mean ± SEM from at least three independent experiments.

was initiated by addition of pNPP (ranging from 0.2 to 5 K_M) to a reaction mixture containing different phosphatases and various fixed concentrations of inhibitors, and stopped by the addition of 1 m NaOH. The inhibition constant K_i and inhibition pattern were evaluated by fitting the data to the Michaelis–Menten equation (or Lineweaver–Burk equation) for competitive inhibition [Eq. (2)–(3)], using linear regression and GraphPad Prism as follows:

$$1/v = K_{Mobs}/(V_{max} \times [\text{Substrate}]) + 1/V_{max} \qquad (2)$$

$$K_{Mobs} = K_M(1 + [\text{Inhibitor}]/K_i) \qquad (3)$$

Cell culture and Immunoblotting. PC12 cells were cultured as previously described.[8b] Cells were preincubated with 5 μm (final concentration) inhibitor (**D3**) or DMSO for 45 min, and then stimulated with 100 ng mL^{-1} NGF for 0, 15, or 30 min. The stimulation was terminated by transferring cells to ice, followed by the addition of lysis buffer (50 mm Tris pH 7.5, 150 mm NaCl, 10 mm NaF, 2 mm EDTA, 10 % glycerol, 1 % NP-40, 0.25 % sodium deoxycholate, 1 mm NaVO$_4$, 1 mm phenylmethylsulfonyl fluoride, 0.3 μm aprotin, 130 μm bestiatin, 1 μm leupeptin, and 1 μm pepstatin) for 15 min. The lysates were then centrifuged at 12 000 rpm for 15 min. The supernatants were collected, and the protein concentrations were measured using a bicinchoninic acid (BCA) protein quantitation kit (Beyotime). Equal amounts of cell lysates were denatured in 2× sodium dodecyl sulfate (SDS) loading buffer and boiled for 10 min. Protein samples were then subjected to western blot analysis with specific anti-phosphocofilin or GAPDH antibodies.

Cell migration assay. PC12 cells were resuspended in Dulbecco's Modified Eagle's Medium (DMEM, serum free) and treated with compound **D3**, **A14**, or control vehicle (0.2 % DMSO) for 45 min. Approximately $1 \times 10^5 / 100$ μL cells were added to each upper chamber (BD Bioscience). The lower chamber contained culture medium with 100 ng mL^{-1} NGF as a chemoattractant. After 24 h, unmigrated cells were removed, and the inserts were fixed with 4 % paraformaldehyde and stained with crystal violet. Then, eight randomly selected high-power fields (HPFs) per insert were used to quantify the number of migrated cells. Each experiment was re-

peated at least in triplicate. Data analysis was conducted with GraphPad Prism software.

Data analysis and software. The data were analyzed using ImageJ and GraphPad Prism software. All experiments were performed in triplicate, and the data are expressed as mean ± SD. Statistical comparisons were performed with ANOVA tests using GraphPad Prism 5.

Acknowledgements

[1] a) M. C. Buss, M. Remke, J. Lee, K. Gandhi, M. J. Schniederjan, M. Kool, P. A. Northcott, S. M. Pfister, M. D. Taylor, R. C. Castellino, *Oncogene* **2015**, *34*, 1126 – 1140; b) A. G. Gilmartin, T. H. Faitg, M. Richter, A. Groy, M. A. Seefeld, M. G. Darcy, X. Peng, K. Federowicz, J. S. Yang, S. Y. Zhang, E. Minthorn, J. P. Jaworski, M. Schaber, S. Martens, D. E. McNulty, R. H. Sinnamon, H. Zhang, R. B. Kirkpatrick, N. Nevins, G. L. Cui, B. Pietrak, E. Diaz, A. Jones, M. Brandt, B. Schwartz, D. A. Heerding, R. Kumar, *Nat. Chem. Biol.* **2014**, *10*, 181; c) C. Pan, H. D. Liu, Z. Gong, X. Yu, X. B. Hou, D. D. Xie, X. B. Zhu, H. W. Li, J. Y. Tang, Y. F. Xu, J. Q. Yu, L. Y. Zhang, H. Fang, K. H. Xiao, Y. G. Chen, J. Y. Wang, Q. Pang, W. Chen, J. P. Sun, *Sci. Rep.* **2013**, *3*, 2333; d) H. M. Wang, Y. F. Xu, S. L. Ning, D. X. Yang, Y. Li, Y. J. Du, F. Yang, Y. Zhang, N. Liang, W. Yao, L. L. Zhang, L. C. Gu, C. J. Gao, Q. Pang, Y. X. Chen, K. H. Xiao, R. Ma, X. Yu, J. P. Sun, *Cell Res.* **2014**, *24*, 1067 – 1090; e) L. Zhang, L. H. Chen, H. Wan, R. Yang, Z. Wang, J. Feng, S. Yang, S. Jones, S. Wang, W. Zhou, H. Zhu, P. J. Killela, J. Zhang, Z. Wu, G. Li, S. Hao, Y. Wang, J. B. Webb, H. S. Friedman, A. H. Friedman, R. E. McLendon, Y. He, Z. J. Reitman, D. D. Bigner, H. Yan, *Nat. Genet.* **2014**, *46*, 726 – 730; f) E. Barone, S. Mosser, P. C. Fraering, *Biochim. Biophys. Acta* **2014**, *1842*, 2500 – 2509; g) E. Ruark, K. Snape, P. Humburg, C. Loveday, I. Bajrami, R. Brough, D. N. Rodrigues, A. Renwick, S. Seal, E. Ramsay, V. Duarte Sdel, M. A. Rivas, M. Warren-Perry, A. Zachariou, A. Campion-Flora, S. Hanks, A. Murray, N. Ansari Pour, J. Douglas, L. Gregory, A. Rimmer, N. M. Walker, T. P. Yang, J. W. Adlard, J. Barwell, J. Berg, A. F. Brady, C. Brewer, G. Brice, C. Chapman, J. Cook, R. Davidson, A. Donaldson, F. Douglas, D. Eccles, D. G. Evans, L. Greenhalgh, A. Henderson, L. Izatt, A. Kumar, F. Lalloo, Z. Miedzybrodzka, P. J. Morrison, J. Paterson, M. Porteous, M. T. Rogers, S. Shanley, L. Walker, M. Gore, R. Houlston, M. A. Brown, M. J. Caufield, P. Deloukas, M. I. McCarthy, J. A. Todd, C. Turnbull, J. S. Reis-Filho, A. Ashworth, A. C. Antoniou, C. J. Lord, P. Donnelly, N. Rahman, *Nature* **2013**, *493*, 406 – 410; h) O. N. Demidov, C. Kek, S. Shreeram, O. Timofeev, A. J. Fornace, E. Appella, D. V. Bulavin, *Oncogene* **2007**, *26*, 2502 – 2506; i) N. Krishnan, D. Koval, D. H. Miller, B. Xue, S. D. Akshinthala, J. Kragelj, M. R. Jensen, C. M. Gauss, R. Page, M. Blackledge, S. K. Muthuswamy, W. Peti, N. K. Tonks, *Nat. Chem. Biol.* **2014**, *10*, 558 – 566; j) A. Emelyanov, D. V. Bulavin, *Oncogene* **2015**, *34*, 4429 – 4438.

[2] a) Y. Wang, Y. Kuramitsu, T. Kitagawa, B. Baron, S. Yoshino, S. Maehara, Y. Maehara, M. Oka, K. Nakamura, *Cancer Lett.* **2015**, *360*, 171 – 176; b) J. Soosairajah, S. Maiti, O. Wiggan, P. Sarmiere, N. Moussi, B. Sarcevic, R.

Sampath, J. R. Bamburg, O. Bernard, *EMBO J.* **2005**, *24*, 473–486; c) T. Ei-seler, H. Doppler, I. K. Yan, K. Kitatani, K. Mizuno, P. Storz, *Nat. Cell Biol.* **2009**, *11*, 545–556; d) Y. Horita, K. Ohashi, M. Mukai, M. Inoue, K. Mizuno, *J. Biol. Chem.* **2008**, *283*, 6013–6021.

[3] S. Dai, P. D. Sarmiere, O. Wiggan, J. R. Bamburg, D. Zhou, *Cell. Microbiol.* **2004**, *6*, 459–471.

[4] X. Hou, R. Li, K. Li, X. Yu, J. P. Sun, H. Fang, *J. Med. Chem.* **2014**, *57*, 9309–9322.

[5] a) H. Bielig, K. Lautz, P. R. Braun, M. Menning, N. Machuy, C. Brugmann, S. Barisic, S. A. Eisler, M. Andree, B. Zurek, H. Kashkar, P. J. Sansonetti, A. Hausser, T. F. Meyer, T. A. Kufer, *PLoS Pathog.* **2014**, *10*, e1004351; b) T. Y. Huang, C. DerMardirossian, G. M. Bokoch, *Curr. Opin. Cell Biol.* **2006**, *18*, 26–31; c) R. Niwa, K. Nagata-Ohashi, M. Takeichi, K. Mizuno, T. Uemura, *Cell* **2002**, *108*, 233–246; d) M. Endo, K. Ohashi, Y. Sasaki, Y. Goshima, R. Niwa, T. Uemura, K. Mizuno, *J. Neurosci.* **2003**, *23*, 2527–2537; e) Y. T. Zhang, D. Y. Ouyang, L. H. Xu, Q. B. Zha, X. H. He, *J. Cell. Biochem.* **2013**, *114*, 2415–2429; f) X. Xu, N. Gera, H. Li, M. Yun, L. Zhang, Y. Wang, Q. J. Wang, T. Jin, *Mol. Biol. Cell* **2015**, *26*, 874–886; g) K. Nagata-Ohashi, Y. Ohta, K. Goto, S. Chiba, R. Mori, M. Nishita, K. Ohashi, K. Kousaka, A. Iwa-matsu, R. Niwa, T. Uemura, K. Mizuno, *J. Cell Biol.* **2004**, *165*, 465–471;

h) J. Ng, L. Luo, *Neuron* **2004**, *44*, 779–793; i) J. W. Zhao, M. R. Zhang, Q. Y. Ji, F. J. Xing, L. J. Meng, Y. Wang, *Molecules* **2012**, *17*, 14975–14994; j) K. Mizuno, *Cell. Signalling* **2013**, *25*, 457–469.

[6] M. Endo, K. Ohashi, K. Mizuno, *J. Biol. Chem.* **2007**, *282*, 13692–13702.

[7] K. Xiao, J. Sun, J. Kim, S. Rajagopal, B. Zhai, J. Villen, W. Haas, J. J. Kovacs, A. K. Shukla, M. R. Hara, M. Hernandez, A. Lachmann, S. Zhao, Y. Lin, Y. Cheng, K. Mizuno, A. Ma'ayan, S. P. Gygi, R. J. Lefkowitz, *Proc. Natl. Acad. Sci. USA* **2010**, *107*, 15299–15304.

[8] a) C. Pan, J. Y. Tang, Y. F. Xu, P. Xiao, H. D. Liu, H. A. Wang, W. B. Wang, F. G. Meng, X. Yu, J. P. Sun, *Sci. Rep.* **2015**, *5*, 8560; b) R. Li, D. D. Xie, J. H. Dong, H. Li, K. S. Li, J. Su, L. Z. Chen, Y. F. Xu, H. M. Wang, Z. Gong, G. Y. Cui, X. Yu, K. Wang, W. Yao, T. Xin, M. Y. Li, K. H. Xiao, X. F. An, Y. Huo, Z. G. Xu, J. P. Sun, Q. Pang, *J. Neurochem.* **2014**, *128*, 315–329.

[9] F. C. Brown, C. K. Bradsher, E. C. Morgan, M. Tetenbaum, P. Wilder, Jr., *J. Am. Chem. Soc.* **1956**, *78*, 384.